FEBS Letters 585 (2011) 3587–3592

journal homepage: www.FEBSLetters.org

The structure of active opsin as a basis for identification of GPCR agonists by dynamic homology modelling and virtual screening assays

Michael Schneider [a,1], Steffen Wolf [a,b], Jürgen Schlitter [a], Klaus Gerwert [a,b,*]

[a] Department of Biophysics, University of Bochum, 44780 Bochum, Germany
[b] CAS-MPG Partner Institute for Computational Biology, Shanghai Institutes of Biological Sciences, 200031 Shanghai, China

ARTICLE INFO

Article history:
Received 4 July 2011
Revised 30 September 2011
Accepted 14 October 2011
Available online 21 October 2011

Edited by Robert B. Russell

Keywords:
Molecular dynamics simulations
GPCR
Dynamic homology model
Beta(2) adrenoreceptor
Opsin
Virtual ligand screening

ABSTRACT

Most of the currently available G protein-coupled receptor (GPCR) crystal structures represent an inactive receptor state, which has been considered to be suitable only for the discovery of antagonists and inverse agonists in structure-based computational ligand screening. Using the β_2-adrenergic receptor (B2AR) as a model system, we show that a dynamic homology model based on an "active" opsin structure without further incorporation of experimental data performs better than the crystal structure of the inactive B2AR in finding agonists over antagonists/inverse agonists. Such "active-like state" dynamic homology models can therefore be used to selectively identify GPCR agonists in in silico ligand libraries.

1. Introduction

G-protein coupled receptors (GPCRs), a versatile superfamily of transmembrane proteins, play a major role in signal transduction and are activated by a diverse set of signals, including small molecules, peptides and light [1]. Around 45% of all drugs on the market modulate the activity of GPCRs [2]. Despite their pharmaceutical importance, only seven GPCRs are available as crystal structures up to now [3–8]. To overcome the lack in structural information on other GPCRs for virtual ligand screening, homology modelling is usually applied [9,10]. From their pharmacological effects, GPCR targeting ligands can be generally divided into agonists, antagonists and inverse agonists [11]. An early discrimination of the investigated ligands into these categories in silico is of high importance for pharmaceutical research. Most GPCR crystal structures represent an inactive state which has been considered to be capable for the discovery of antagonists and inverse agonists only [12–14]. To date, only the structure of opsin [15] and most recently structural models of active conformations of the β_2-adrenergic receptor (B2AR) [16–18], the agonist-bound β_1-adrenergic receptor [19] and a constitutively active rhodopsin [20] could be potentially used as a template for the modelling of active GPCRs and subsequent virtual screening for agonists. In this work, we want to test how far this "active state" structural information can be exploited to discover the structures of agonists in preference over antagonists/inverse agonists with B2AR as a model system.

We used the opsin crystal structure as a template to model an activated state of the β_2-adrenergic receptor, which is well characterized by many biochemical studies [21]. A similar approach was used recently by Simpson et al. [22]. In contrast to their study, we do explicitly not include additional experimental data on the receptor of interest to verify the general applicability of our approach. Furthermore, our modelling procedure takes the dynamics of receptor and ligand into account, without constraints on the helical backbone, but within a native membrane model. The model was constructed by dynamic homology modelling [9]. We modelled the activated state in its apo form and in complex with an agonist (epinephrine) and an inverse agonist (carazolol). For comparison, we also introduced those ligands into the inactive state crystal structure of B2AR (PDB ID 2RH1) [5]. Dynamics of the protein/ligand complexes were investigated by free MD simulations in

Abbreviations: B2AR, (inactive) β_2-adrenergic receptor; B2AR*, active β_2-adrenergic receptor; EF, enrichment factor; GPCR, G protein coupled receptor; IFP, interaction fingerprint; tIFP, Tanimoto coefficient derived from IFPs; VLS, virtual ligand screening; MD, molecular dynamics; RMSD, root mean square deviation; ROC, receiver operator curve

* Corresponding author at: Department of Biophysics, University of Bochum, 44780 Bochum, Germany. Fax: +49 234 3214626.
E-mail addresses: swolf@bph.rub.de (S. Wolf), gerwert@bph.rub.de (K. Gerwert).
[1] Present address: Technische Universität Berlin, 10623 Berlin, Germany.

0014-5793/$36.00
doi:10.1016/j.febslet.2011.10.027

an explicit membrane/solvent environment. Representative binding modes that exhibit the major protein/ligand contacts are extracted by hierarchical clustering of interaction fingerprints (IFPs) [23] of MD snapshots. The model of the activated state was evaluated in virtual screening experiments, using the representative binding mode of the activated state as a reference to rescore the virtual screening results by IFPs.

2. Materials and methods

Model construction and MD simulations, the application of interaction fingerprints in MD simulations, the preparation of ligand database and the virtual screening protocol and analysis are described in detail in the Supplementary data available online.

3. Results and discussion

3.1. Stability of the active-state receptor model

Fig. 1 shows the root mean square displacement of the Cα atoms of the 7TM domain (Cα-RMSD) from the initial structure of both models during 70 ns of MD simulation. The apo form of the inactive model (B2AR) deviates the most from its starting structure (Fig. 1A). Both kinds of ligands stabilize the receptor to the same extends. This finding supports the idea that the crystal structure 2RH1 represents a partially activated state of the receptor [24]. Fig. 1 B shows the RMSD from the starting structure for the model of the activated receptor (B2AR*). Clearly, the apo form of the receptor diverges most from the initial structure during the simulation. The epinephrine bound model stays closer to the starting structure than does the carazolol bound model. Kobilka and Deupi [25] proposed that agonists stabilize the activated receptor and hence shift the equilibrium of activated and inactivated states toward the active conformation. Our finding agrees well with this hypothesis.

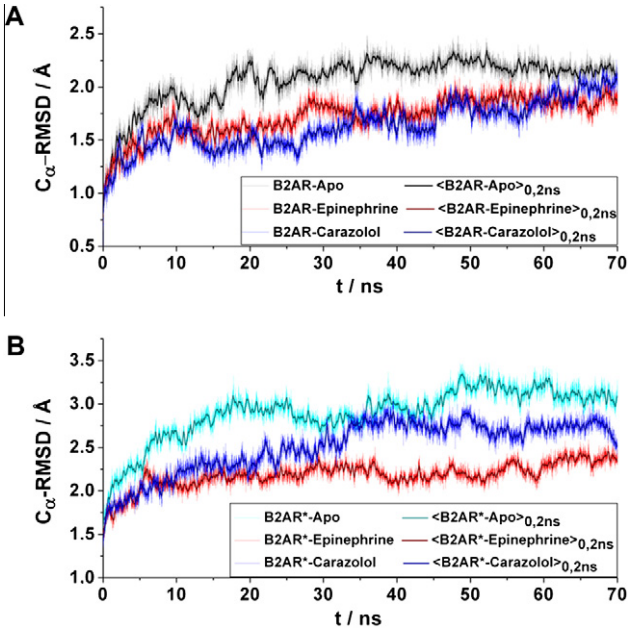

Fig. 1. Cα-RMSD comparison of the 7TM domain of B2AR and B2AR* (apo form, epinephrine bound and carazolol bound, respectively) to their initial structures during 70 ns MD simulation. (A) Cα-RMSD of B2AR during the simulation. The RMSD of B2AR-apo (gray) reaches a maximum of 2.2 Å after 20 ns. The RMSD of B2AR-epinephrine (red) fluctuates between 1.8 and 2.0 Å. The RMSD of B2AR-carazolol (blue) rises to a maximum of 2.0 Å during the simulation. Both kinds of ligands stabilize the receptor to the same extend. (B) Cα-RMSD of the B2AR* structures during the simulation. The RMSD of B2AR*-apo (cyan) remains between 3.1 and 3.2 Å after 50 ns. The RMSD of B2AR*-epinephrine (red) rises to 2.2 Å after the first 6 ns. B2AR*-carazolol (blue) attains a RMSD of 2.8 Å after the first 35 ns. The model structures of the activated receptor are stable during the MD simulations. Epinephrine stabilizes the B2AR* structure better than carazolol.

We also compared our model with the recently published structures of an active state of B2AR [16,18]. We find that the 7TM domain is in good agreement with the crystal structures (Fig. S1). During the last 5 ns of simulation, the average Cα-RMSD between the model and both structures is 2.2 Å. While helix I to IV are in excellent agreement (RMSD about 1 Å), helices V to VII deviate up to 3.0 Å from their position in the active state crystal structure. The outward movement of the intracellular side of helix VI, defined by the opsin structure, is less pronounced in the model than in the active B2AR crystal structures, indicating that the opsin structure might not resemble a fully activated GPCR state [15], or that the extend of this movement during activation is different between the two receptors.

3.2. Dynamic ligand binding

To analyse ligand binding in detail, we looked closer at the dynamics of ligand binding and extracted information on the dynamics of binding modes, which can be used to characterize the major molecular features of the receptor–ligand interactions. As the formation of an active GPCR state involve conformational changes in the ligand binding pocket [16], agonists and antagonists/inverse agonists will have different contacts with the binding pocket, as they are thought to stabilize active and inactive conformations, respectively. We here monitor dynamic ligand binding by interaction fingerprints (IFP) [23,26,27], which are a binary pattern of protein/ligand contacts. They can also readily be used to monitor ligand interactions with the receptor during MD simulations. IFPs, which map the protein/ligand interactions, are therefore a suitable tool to discriminate between the interaction pattern of ligands in an inactive and an active receptor, and thus between agonists and antagonists as well. We extracted a snapshot from the MD trajectory each 5 ps and computed the IFP from the structure. Each IFP is a bit string that consists of 7 interaction types per residue in the binding pocket.: Hydrophobic interactions, aromatic face-to-edge, aromatic face-to-face, H-Bond donor, H-Bond acceptor, ionic bond to negatively charged residue and ionic bond to positively charged residue. A bit is set to 1 if the respective interaction is observed between the ligand and the receptor in a snapshot. The resulting IFPs were clustered by hierarchical clustering. From the resulting clusters, we selected the most populated cluster (present in >65% of simulated time). A representative IFP for this cluster was constructed by setting each bit to 1 if its interactions were present in at least 50% of the IFPs in that particular cluster (see Supplementary data for details). These representative IFPs are later used as "reference IFPs" for scoring of the VLS results. This approach provides a straightforward and systematic method to extract major binding features from the MD trajectory.

Fig. 2 shows representatives of the dynamic binding modes of carazolol and epinephrine obtained from simulations of the inactive and active receptor. Each image of the two ligands shows a snapshot from the MD trajectories, whose ligand–receptor interactions match their representative IFP to a maximal extend. Although representing an average binding mode by construction, and the exact binding contacts of the representative IFP do not necessarily need to be actually present all at once in the MD trajectory, this is the case for the structures presented here.

A thorough discussion of the respective binding modes can be found in the Supplementary data section. In general, epinephrine is more mobile than carazolol within both receptor models, most probably because of the smaller size of its aromatic ring. It probes

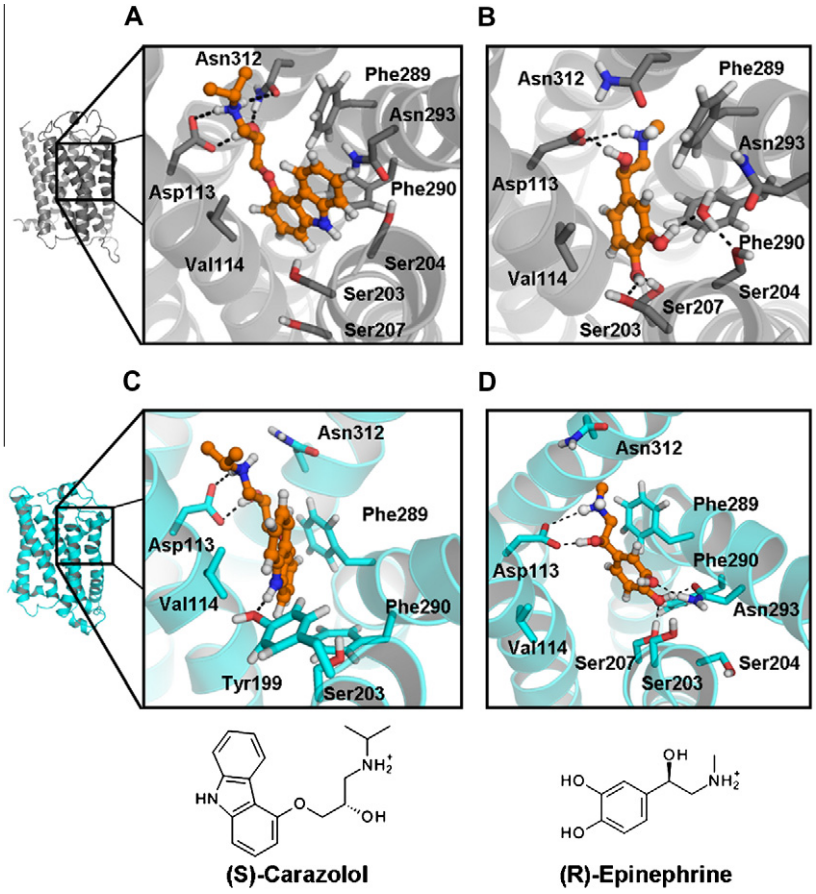

Fig. 2. Representative binding modes of carazolol (inverse agonist) and epinephrine (agonist) after 20 ns MD simulation. (A, B) Inactive receptor model B2AR (based on 2RH1). (C, D) active receptor model B2AR*. (A) Carazolol is overall employing the same binding mode as in the crystal structure 2RH1. (B) The para-hydroxyl group of epinephrine is hydrogen bonding to 203 and is accepting a hydrogen bond from Ser207. The meta-hydroxyl group is hydrogen bonding to Ser204 and Asn293 over a water mediated hydrogen bond. (C) Carazolol is shifting along helix V towards the extracellular side in B2AR*. The cabazole nitrogen atom is hydrogen bonding Tyr199. (D) Binding mode of epinephrine in B2AR*. Ser207 hydrogen bonds the para-hydroxyl group, which also acts as a donor to Asn293. Asn293 is also hydrogen bonding the meta-hydroxyl group. The clamp-like connection of the ethanolammonium group and Asp113 is a consistent feature of all ligand–receptor pairs.

different locations in the binding pocket (compare Fig. 2 and S2), which results in a less frequent observation of certain contacts. This observation is in good agreement with the lower binding energy of epinephrine compared to carazolol, resulting in a much lower experimentally determined affinity of epinephrine compared to carazolol (μM vs. pM range) [5,28]. The receptor/ligand contacts of the inactive receptor agree well with experimental data and earlier MD studies [4,29–31].

Fig. 2C and D show the dynamic binding modes of carazolol and epinephrine in B2AR*, respectively. In B2AR*, carazolol is much more mobile than in B2AR and loses many binding features that are present in the ground state structure of B2AR (2RH1) [5]. We assume that this binding mode is an artificial state, containing an inverse agonist in an active-like receptor state. Epinephrine's dynamic binding mode in B2AR* agrees well with experimental and theoretical data available [16,28,30,32,33]. Summing up, the dynamic binding modes of both ligands in both models thus are in good agreement with data from earlier MD and experimental investigations. Our in silico dynamic homology modelling strategy will therefore most likely result in protein/ligand interactions, which are comparable to the ones in vitro/in vivo. We can use the simulations of epinephrine and carazolol to determine reference IFPs for agonists and antagonists/inverse agonists, and apply them to rescore docking positions of other ligands to discriminate them into agonists and antagonists/inverse agonists. The good agreement with experimental data suggests that our approach might be suitable to investigate the binding modes of ligands of other GPCRs as active state dynamic homology models, which are less studied than B2AR, as well.

3.3. Virtual ligand screening verifies activated receptor model

To verify whether the active structure model is capable to harbour other agonists, we challenged it in a virtual ligand screening (VLS) experiment. We tested its ability to retrieve experimentally known agonists and to discriminate them from antagonists and inverse agonists.

For this purpose, we compiled a test set of known B2AR ligands, containing 20 antagonists/inverse agonists and 20 agonists, and 960 randomly chosen decoy structures. The decoy set was further filtered to ensure that the decoys are capable to fit into the binding pocket and have no negative charge, which would result in repulsion from Asp113, resulting in 773 decoys (see Supplementary data for details). The entire test set was then docked into the B2AR/B2AR* receptor structures using Autodock Vina [34]. Note that we only needed to extract four snapshots from the first 20 ns on MD simulations for docking, as the development of protein/ligand contacts in the ligand binding pocket is completed within the first 5 ns of simulation (see Supplementary data for further information). To obtain a quantitative criterion to discriminate between agonists and antagonists/inverse agonists, we calculated the IFP for each binding pose and compared it to the corresponding

reference IFP. Reference IFPs were calculated from the dynamic binding modes of epinephrine and carazolol in B2AR* and B2AR (see methods for details). As a measure of similarity, we used the Tanimoto coefficient [35] as a ligand score (tIFP). tIFPs were shown to be effective in other VLS studies with inactive GPCR models [27,36]. Only the highest scoring pose for each ligand was considered for the final ranking and discrimination into pharmacological classes. Ligands were ranked by their Tanimoto coefficient to the reference IFP (highest first). High coefficients indicate that the binding mode of the ligand exhibits many interactions that are also present in the reference IFP.

Fig. 3 shows the obtained ligand poses for the antagonists/inverse agonists (r)-pindolol, (r)-timolol and (s)-CGP-12177, and for the agonists (s)-reproterol, (s)-pirbuterol and (r)-dobutamine. Note that the antagonists/inverse agonists were docked into the inactive receptor models and the agonists into the activated receptor models. The ligands fit nicely into the binding pocket. Scores and ranks for the ligand poses in Fig. 3 are given in Table S1. While agonists could easily be docked into the protein, the Autodock exhaustive parameter needed to be increased 10-fold to give good poses for antagonists and inverse agonists. It emerges that scoring the ligand by tIFP is mandatory to receive good rankings for the experimentally known ligands. Antagonists/inverse agonists are reasonably well scored by the native scoring function of Vina: e.g. carazolol, the ligand in the crystal structure 2RH1, is assigned rank 10 with a predicted energy of −10.6 kcal/mol and CGP-12177 is ranked 38 with −9.4 kcal/mol. However, pindolol and timolol score much poorer, obtaining the ranks 134 and 885, respectively. Scoring by tIFP drastically improves the ranking: the antagonist/inverse agonist poses in Fig. 3 are ranked among the first 20 places. This trend is even stronger for agonists, most of which are ranked poorly by the native Vina scoring function. Vina's scoring function is optimized towards experimentally measured affinities [34]. However, some ligands, including the native agonist epinephrine, bind with micromolar affinity to B2AR [28,37]. Therefore, the affinity of a particular GPCR ligand does not always coincide with its ability to activate the receptor. Furthermore, as docking means trying to place ligands into binding cavities, which from their form are not optimized to specifically incorporate them, affinities determined in silico may be wrong. We assume that ligands with similar activation properties (e.g. agonists) also share similar protein–ligand interaction patterns, which can be quantified by using our tIFP scheme. A nice example for the power of our approach is (r)-pindolol: though it binds with nanomolar affinity to B2AR, it is scored poorly by the Vina scoring function. Nevertheless, the antagonist-defining protein/ligand contacts are already present, so that out tIFP scheme identifies (r)-pindolol as antagonist/inverse agonist. Hence, while searching for an affine ligand does not necessarily lead to an activating ligand, this lack in information can be overcome by applying our tIFP scheme. We have to mention that though pindolol can also be seen as a partial agonist [30], we cannot identify it as such with our approach. The structural differences between a partial agonist-bound and an antagonist-bound receptor seem to be too subtle to be recognized by our method. Nevertheless, our approach correctly identifies pindolol as antagonist instead of as (full) agonist.

Fig. 4 A shows enrichment factors (EF) for all VLS experiments for the 0.5%, 1% and 2% top-scoring ligands, respectively. Note that Fig. 4 shows the data for the filtered decoy set (see Supplementary data for details). Virtual screening results for the unfiltered decoy set are shown in the Supplementary data (Fig. S5). EF is defined as the fractions of compounds with desired properties found divided by the fraction of the full library screened (see Supplementary data for details). By the means of EFs, the active (B2AR*) receptor model outperforms the inactive model (B2AR) in retrieving agonists. The moderate EF of B2AR for agonists agrees well with

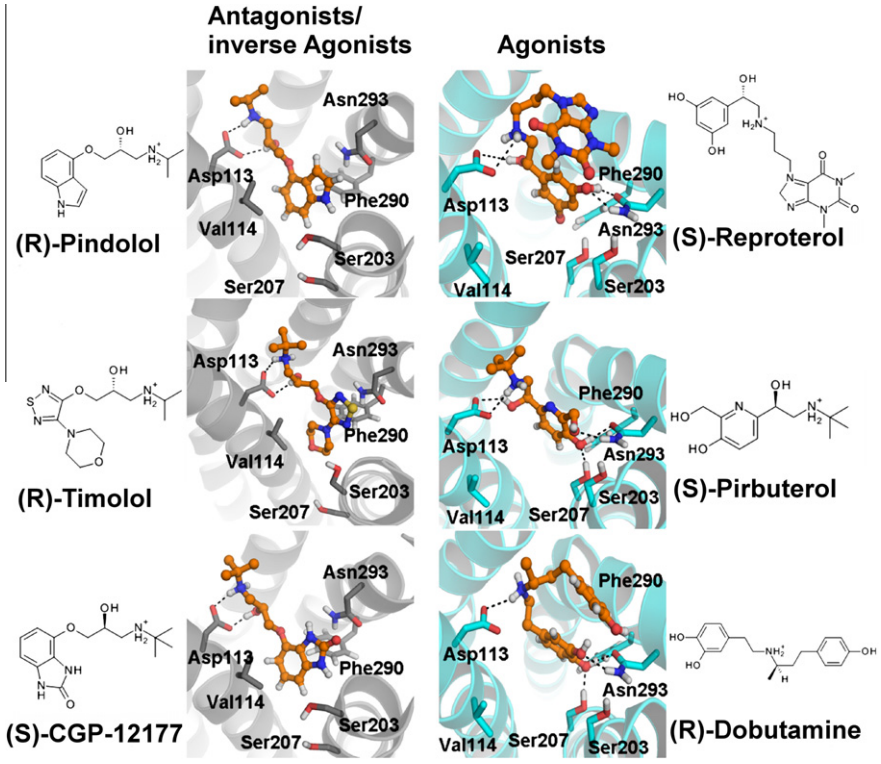

Fig. 3. Exemplary docking poses of antagonists/inverse agonists (left panel) and agonists (right panel). Antagonists/inverse agonists were docked into structures of the B2AR-carazolol simulation, agonists into structures of the B2AR*-epinephrine simulation. The poses shown have been ranked by their tIFP-scores (see ranks and scores in Table S1). Left panel: Antagonists/inverse agonists (s)-pindolol, (r)-timolol and (s)-CGP-12177. Right panel: Agonists (s)-reproterol, (s)-pirbuterol and (r)-dobutamine.

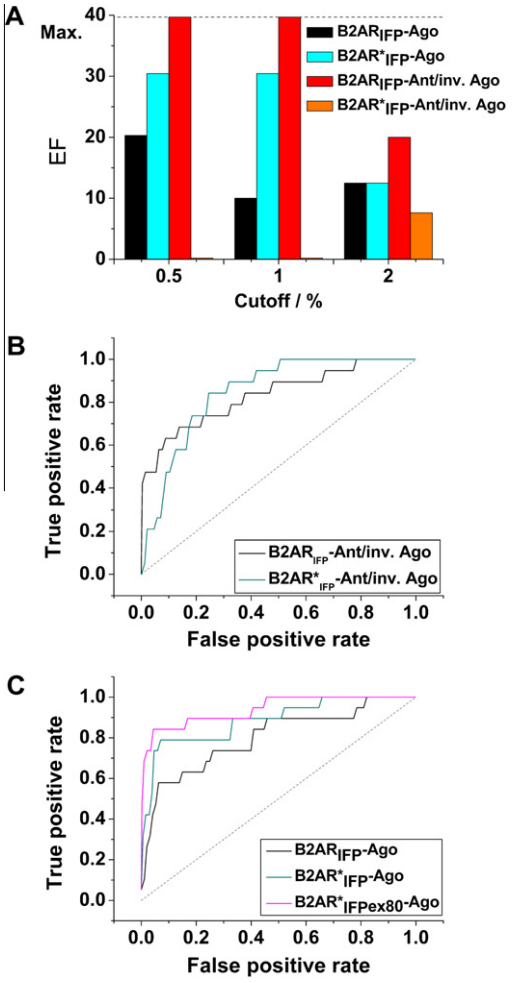

Fig. 4. Performance of the different models in discrimination between agonists and antagonists/inverse agonists. The filtered dataset was used to compute the results for this figure. (A) Enrichment factors (EF) of the VLS experiments for antagonists/inverse agonists and agonists using B2AR and B2AR* as receptor structures. EF values are shown for cutoffs of 0.5%, 1% and 2%. The dotted line indicates the theoretical maximum EF value. Black: EF for agonists docked into B2AR. Cyan: EF for agonists docked into B2AR*. Red: EF for antagonists/inverse agonists docked into B2AR. Orange: EF for antagonists/inverse agonists docked into B2AR*. While B2AR is better capable to find antagonists/inverse agonists in a given ligand library, B2AR* is better suited to find agonists. (B) ROC curves of B2AR (black) and B2AR* (cyan) for antagonists/inverse agonists. The curve of B2AR rises earlier, but the overall course is very similar for B2AR and B2AR*. B2AR performs better in finding antagonists/inverse agonists than B2AR*. (C) ROC curves of B2AR (black) and B2AR* (cyan) for agonists. The ROC curve for B2AR* shows the superior performance of B2AR* to recognize agonists relative to B2AR. Increasing the exhaustiveness parameter leads to even better performance as indicated by the curve in magenta.

the results of other studies [36,38]. Nevertheless, B2AR* displays higher enrichment rates for agonists than B2AR at a cut-off of 0.5% and 1%. It is striking that the opposite is true for antagonists/inverse agonists. This shows that the model of the activated receptor selectively identifies agonists, while the inactive crystal-structure based model is selective for antagonists and inverse agonists. This is an encouraging finding and highlights that dynamic homology modelling using the opsin crystal structure as a template can yield "activated" receptor models of class A GPCRs.

Another way to characterise the VLS results is a receiver operator characteristic (ROC) [39]. We checked in this analysis how many percent of agonists or antagonists/inverse agonists present in a ligand library (true positives) are found at a given percentage of inactive ligands or ligands with undesired effect on the receptor (false positives). Fig. 4B and C show the results of the ROC-analysis. AUC-values (area under ROC curve) are similar for the two cases with 0.81 for B2AR and 0.82 for B2AR*. The course of the curves reveals that antagonists/inverse agonists are higher ranked and thus more readily identified in B2AR than in B2AR*. This shows as well, that B2AR is the more appropriate structure for the identification of antagonists/inverse agonists of the β_2-adrenergic receptor as shown in other recent studies [13]. Fig. 4C shows the ROC-curves for agonists. B2AR* shows superior performance over B2AR for agonists. The ROC-curve of B2AR* rises much faster than the curve of B2AR and a bigger part of all agonists is highly ranked. For all false positive rate values, the ROC-curve of B2AR* lies above or equal relative to the B2AR curve. Hence, B2AR* is much more suitable for the identification of agonists, which is also reflected by the AUC of 0.9. To test whether results can be improved when spending more computational recourses on the search of a suitable ligand pose, we repeated the docking of agonists with a 10-fold increased exhaustiveness value (from 8 to 80), like we did for antagonists/inverse agonists. This enhances the performance even further and leads to an AUC of 0.95 for B2AR*. A ROC-analysis for ranking based on Autodock scores alone is shown in Fig. S6. As can be seen, our IFP scheme outperforms an analysis solely basing on evaluating binding energies in finding suitable ligands as well as classifying them into agonists and antagonists/inverse agonists.

4. Conclusion

This study shows that the active state structure of opsin is suited as a structural basis to identify GPCR agonists without the incorporation of additional experimental data. We need to emphasize that dynamic homology modelling starting from active state GPCR crystal structures does not necessarily produce active state structures, but rather "active-like" models that display characteristics of active GPCRs. Nevertheless, such dynamic homology "active-like" models can be used to selectively find agonists of other GPCRs of interest in structure-based discovery campaigns. Together with models from inactive structures, our method can facilitate the discovery of bioactive lead structures that target GPCRs with a desired effect.

Acknowledgements

We would like to thank T. Rudack and A. Mosig for useful discussion. M.S. acknowledges a fellowship from the German National Academic Foundation. S.W. is funded by a Chinese Academy of Sciences Fellowship for Young International Scientists. K.G. acknowledges a fellowship of the Mercator foundation. Calculations were performed on the PICB HPC cluster.

Appendix A. Supplementary data

Supplementary data associated with this article can be found, in the online version, at doi:10.1016/j.febslet.2011.10.027.

References

[1] Ballesteros, J., Kitanovic, S., Guarnieri, F., Davies, P., Fromme, B.J., Konvicka, K., Chi, L., Millar, R.P., Davidson, J.S., Weinstein, H. and Sealfon, S.C. (1998) Functional microdomains in G-protein-coupled receptors. The conserved arginine-cage motif in the gonadotropin-releasing hormone receptor. J. Biol. Chem. 273, 10445–10453.
[2] Drews, J. (2000) Drug discovery: a historical perspective. Science 287, 1960–1964.
[3] Okada, T., Sugihara, M., Bondar, A.-N., Elstner, M., Entel, P. and Buss, V. (2004) The retinal conformation and its environment in rhodopsin in light of a new 2.2 Å crystal structure. J. Mol. Biol. 342, 571–583.
[4] Warne, T., Serrano-Vega, M.J., Baker, J.G., Moukhametzianov, R., Edwards, P.C., Henderson, R., Leslie, A.G.W., Tate, C.G. and Schertler, G.F.X. (2008) Structure of a β_1-adrenergic G-protein-coupled receptor. Nature 454, 486–491.
[5] Cherezov, V., Rosenbaum, D.M., Hanson, M.A., Rasmussen, S.G.F., Thian, F.S., Kobilka, T.S., Choi, H.-J., Kuhn, P., Weis, W.I., Kobilka, B.K. and Stevens, R.C.

(2007) High resolution crystal structure of an engineered human β_2-adrenergic G protein-coupled receptor. Science 318, 1258–1265.
[6] Jaakola, V.-P., Griffith, M.T., Hanson, M.A., Cherezov, V., Chien, E.Y.T., Lane, J.R., Ijzerman, A.P. and Stevens, R.C. (2008) The 2.6 Å crystal structure of a human A2A adenosine receptor bound to an antagonist. Science 322, 1211–1217.
[7] Wu, B., Chien, E.Y.T., Mol, C.D., Fenalti, G., Liu, W., Katritch, V., Abagyan, R., Brooun, A., Wells, P., Bi, F.C., Hamel, D.J., Kuhn, P., Handel, T.M., Cherezov, V. and Stevens, R.C. (2010) Structures of the CXCR4 Chemokine GPCR with small-molecule and cyclic peptide antagonists. Science 330, 1066–1071.
[8] Chien, E.Y.T., Liu, W., Zhao, Q., Katritch, V., Won Han, G., Hanson, M.A., Shi, L., Newman, A.H., Javitch, J.A., Cherezov, V. and Stevens, R.C. (2010) Structure of the human dopamine D3 receptor in complex with a D2/D3 selective antagonist. Science 330, 1091–1095.
[9] Wolf, S., Böckmann, M., Höweler, U., Schlitter, J. and Gerwert, K. (2008) Simulations of a G protein-coupled receptor homology model predict dynamic features and a ligand binding site. FEBS Lett. 582, 3335–3342.
[10] Michino, M., Abola, E., Brooks, C.L., Dixon, J.S., Moult, J. and Stevens, R.C. (2009) Community-wide assessment of GPCR structure modeling and docking understanding. Nat. Rev. Drug Discov. 8, 455–463.
[11] Kenakin, T.P. (2008) Pharmacological onomastics: What's in a name? Br. J. Pharmacol. 153, 432–438.
[12] Rosenbaum, D.M., Rasmussen, S.G.F. and Kobilka, B.K. (2009) The structure and function of G-protein-coupled receptors. Nature 459, 356–363.
[13] Kolb, P., Rosenbaum, D.M., Irwin, J.J., Fung, J.J., Kobilka, B.K. and Shoichet, B.K. (2009) Structure-based discovery of β_2-adrenergic receptor ligands. Proc. Natl. Acad. Sci. USA 106, 6843–6848.
[14] Archer, E., Maigret, B., Escrieut, C., Pradayrol, L. and Fourmy, D. (2003) Rhodopsin crystal: new template yielding realistic models of G-protein-coupled receptors? Trends Pharmacol. Sci. 24, 36–40.
[15] Scheerer, P., Park, J.H., Hildebrand, P.W., Kim, Y.J., Krausz, N., Choe, H.-W., Hofmann, K.P. and Ernst, O.P. (2008) Crystal structure of opsin in its G-protein-interacting conformation. Nature 455, 497–502.
[16] Rasmussen, S.G.F., Choi, H.-J., Fung, J.J., Pardon, E., Casarosa, P., Chae, P.S., DeVree, B.T., Rosenbaum, D.M., Thian, F.S., Kobilka, T.S., Schnapp, A., Konetzki, I., Sunahara, R.K., Gellman, S.H., Pautsch, A., Steyaert, J., Weis, W.I. and Kobilka, B.K. (2011) Structure of a nanobody-stabilized active state of the β_2 adrenoceptor. Nature 469, 175–180.
[17] Rosenbaum, D.M., Zhang, C., Lyons, J.A., Holl, R., Aragao, D., Arlow, D.H., Rasmussen, S.G.F., Choi, H.-J., DeVree, B.T., Sunahara, R.K., Chae, P.S., Gellman, S.H., Dror, R.O., Shaw, D.E., Weis, W.I., Caffrey, M., Gmeiner, P. and Kobilka, B.K. (2011) Structure and function of an irreversible agonist β_2 adrenoceptor complex. Nature 469, 236–240.
[18] Rasmussen, S.G.F., DeVree, B.T., Zou, Y., Kruse, A.C., Chung, K.Y., Kobilka, T.S., Thian, F.S., Chae, P.S., Pardon, E., Calinski, D., Mathiesen, J.M., Shah, S.T.A., Lyons, J.A., Caffrey, M., Gellman, S.H., Steyaert, J., Skiniotis, G., Weis, W.I., Sunahara, R.K. and Kobilka, B.K. (2011) Crystal structure of the β2 adrenergic receptor-Gs protein complex. Nature 477, 549–555.
[19] Warne, T., Moukhametzianov, R., Baker, J.G., Nehmé, R., Edwards, P.C., Leslie, A.G.W., Schertler, G.F.X. and Tate, C.G. (2011) The structural basis for agonist and partial agonist action on a β_1-adrenergic receptor. Nature 469, 241–244.
[20] Standfuss, J., Edwards, P.C., D'Antona, A., Fransen, M., Xie, G., Oprian, D.D. and Schertler, G.F.X. (2011) The structural basis of agonist-induced activation in constitutively active rhodopsin. Nature 471, 656–660.
[21] Pierce, K.L., Premont, R.T. and Lefkowitz, R.J. (2002) Seven-transmembrane receptors. Nat. Rev. Mol. Cell Biol. 3, 639–650.
[22] Simpson, L.M., Wall, I.D., Blaney, F.E. and Reynolds, C.A. (2011) Modeling GPCR active state conformations: The β_2-adrenergic receptor. Proteins 79, 1441–1457.
[23] Deng, Z., Chuaqui, C. and Singh, J. (2004) Structural interaction fingerprint (SIFt): a novel method for analyzing three-dimensional protein−ligand binding interactions. J. Med. Chem. 47, 337–344.
[24] Han, D.S., Wang, S.X. and Weinstein, H. (2008) Active state-like conformational elements in the β_2-AR and a photoactivated intermediate of rhodopsin identified by dynamic properties of GPCRs. Biochemistry 47, 7317–7321.
[25] Kobilka, B.K. and Deupi, X. (2007) Conformational complexity of G-protein-coupled receptors. Trends Pharmacol. Sci. 28, 397–406.
[26] Marcou, G. and Rognan, D. (2007) Optimizing fragment and Scaffold docking by use of molecular interaction fingerprints. J. Chem. Inf. Model. 47, 195–207.
[27] Radestock, S., Weil, T. and Renner, S. (2008) Homology model-based virtual screening for GPCR ligands using docking and target-biased scoring. J. Chem. Inf. Model. 48, 1104–1117.
[28] Liapakis, G., Ballesteros, J.A., Papachristou, S., Chan, W.C., Chen, X. and Javitch, J.A. (2000) The forgotten serine. A critical role for Ser-203$^{5.42}$ in ligand binding to and activation of the β_2-adrenergic receptor. J. Biol. Chem. 275, 37779–37788.
[29] Strader, C.D., Fong, T.M., Tota, M.R., Underwood, D. and Dixon, R.A. (1994) Structure and function of G protein-coupled receptors. Annu. Rev. Biochem. 63, 101–132.
[30] Huber, T., Menon, S. and Sakmar, T.P. (2008) Structural basis for ligand binding and specificity in adrenergic receptors: implications for GPCR-targeted drug discovery. Biochemistry 47, 11013–11023.
[31] Kaszuba, K., Róg, T., Bryl, K., Vattulainen, I. and Karttunen, M. (2010) Molecular dynamics simulations reveal fundamental role of water as factor determining affinity of binding of beta-blocker nebivolol to β_2-adrenergic receptor. J. Phys. Chem. B 114, 8374–8386.
[32] Strader, C.D., Candelore, M.R., Hill, W.S., Sigal, I.S. and Dixon, R.A. (1989) Identification of two serine residues involved in agonist activation of the beta-adrenergic receptor. J. Biol. Chem. 264, 13572–13578.
[33] Pooput, C., Rosemond, E., Karpiak, J., Deflorian, F., Vilar, S., Costanzi, S., Wess, J. and Kirk, K.L. (2009) Structural basis of the selectivity of the β_2-adrenergic receptor for fluorinated catecholamines. Bioorg. Med. Chem. 17, 7987–7992.
[34] Trott, O. and Olson, A.J. (2010) AutoDock Vina: improving the speed and accuracy of docking with a new scoring function, efficient optimization and multithreading. J. Comput. Chem. 31, 455–461.
[35] Tanimoto, T.T. (1957). *IBM Internal Report.*
[36] de Graaf, C. and Rognan, D. (2008) Selective structure-based virtual screening for full and partial agonists of the beta (2) adrenergic receptor. J. Med. Chem. 51, 4978–4985.
[37] Green, S.A., Cole, G., Jacinto, M., Innis, M. and Liggett, S.B. (1993) A polymorphism of the human β_2-adrenergic receptor within the fourth transmembrane domain alters ligand binding and functional properties of the receptor. J. Biol. Chem. 268, 23116–23121.
[38] Reynolds, K.A., Katritch, V. and Abagyan, R. (2009) Identifying conformational changes of the β_2 adrenoceptor that enable accurate prediction of ligand/receptor interactions and screening for GPCR modulators. J. Comput. Aid. Mol. Des. 23, 273–288.
[39] Zou, K.H., O'Malley, A.J. and Mauri, L. (2007) Receiver-operating characteristic analysis for evaluating diagnostic tests and predictive models. Circulation 115, 654–657.